center. The present and following papers represent our initial inquiry into this question.

Acknowledgment. At Rice University this work was supported by National Institutes of Health Grant GM-28451 from the National Institute of General Medical Sciences and Grant C-624 from the Robert A. Welch Foundation. The Rigaku AFC-5S X-ray diffractometer was purchased, in part, through an instrumentation grant from the National Science Foundation. Professor Mike Squillacote is thanked for helpful discussions regarding molecular mechanics and NMR spectroscopy.

Registry No. $[Zn^{II}((5\text{-MeimidH})_2DAP)](BF_4)_2$, 131702-91-5; $[Zn^{II}((imidH)_2DAP)](BF_4)_2$, 82135-49-7; $[Zn^{II}((py)_2DAP)](BF_4)_2$, 94629-92-2; $[Cu^{II}((5\text{-MeimidH})_2DAP)](BF_4)_2$, 131702-93-7; $[Cu^{I}((5\text{-MeimidH})_2DAP)](BF_4)$, 131726-89-1; $[Cu^{I}((imidH)_2DAP)](BF_4)$, 131726-90-4; $[Cu^{I}((py)_2DAP)](BF_4)$, 131702-94-8; 4-(carboethoxy)-5-methylimidazole, 51605-32-4; 5-methyl-4-(hydroxymethyl)imidazole hydrochloride, 38585-62-5; 5-methyl-4-(chloromethyl)imidazole hydrochloride, 51605-33-5; 5-methyl-4-(cyanomethyl)imidazole, 51667-66-4; 5-methylhistamine, 36507-31-0; 2,6-diacetylpyridine, 1129-30-2.

Supplementary Material Available: Tables S-II-S-V, listing anisotropic thermal parameters, hydrogen atom coordinates, rigid group parameters, and the calculated least-squares planes for $[Zn^{II}((5\text{-MeimidH})_2DAP)](BF_4)_2$, Table S-VI, listing temperature-dependent NMR data for $[Zn^{II}((5\text{-MeimidH})_2DAP)]^{2+}$, $[Zn^{II}((imidH)_2DAP)]^{2+}$, and $[Zn^{II}((py)_2DAP)]^{2+}$ in CD_3CN and acetone-d_6, $[Cu^{I}((5\text{-MeimidH})_2DAP)]^{+}$ in CD_2Cl_2 and CD_3CN, and $[Cu^{I}((imidH)_2DAP)]^{+}$ in CD_3CN, Figure S-1, showing the package diagram for $[Zn^{II}((5\text{-MeimidH})_2DAP)](BF_4)_2$, and Figure S-2, giving the simulated ^1H NMR spectrum of the methylene region for $[Cu^{I}((py)_2DAP)]^{+}$ (20 pages); Table S-I, listing observed and calculated structure amplitude factors (×10) for $[Zn^{II}((5\text{-MeimidH})_2DAP)](BF_4)_2$ (20 pages). Ordering information is given on any current masthead page.

Contribution from the Department of Chemistry and Laboratory for Biochemical and Genetic Engineering, William Marsh Rice University, P.O. Box 1892, Houston, Texas 77251, and Departments of Chemistry, University of Notre Dame, Notre Dame, Indiana 46556, and Auburn University, Auburn, Alabama 36849

An Electron Self-Exchange Study of the Coordination-Number-Invariant Pentacoordinate Copper(I/II) Couple $[Cu^{I,II}((5\text{-MeimidH})_2DAP)]^{+/2+}$ [1]

DeAnna K. Coggin,[2] Jorge A. González,[2] Alan M. Kook,[2] Carmen Bergman,[3] Theodore D. Brennan,[3] W. Robert Scheidt,*[,3] David M. Stanbury,*[,4] and Lon J. Wilson*[,2]

Received July 3, 1990

The electron self-exchange rate of the $[Cu^{I,II}((5\text{-MeimidH})_2DAP)]^{+/2+}$ cation couple has been determined in CD_3CN, as a function of temperature, by dynamic NMR line-broadening techniques. Under anaerobic conditions with μ = 25 mM ($(CH_3)_4NBF_4$), the rate constant ranged from 0.8×10^4 (243 K) to 3.5×10^4 M^{-1} s^{-1} (293 K). From the temperature dependence of the self-exchange rate, activation parameters of $\Delta H^* = 16.2 \pm 3.3$ kJ mol^{-1} and $\Delta S^* = -103 \pm 12$ J K^{-1} mol^{-1} have been obtained. An X-ray crystal structure of the $[Cu^{II}((5\text{-MeimidH})_2DAP)]^{2+}$ cation shows the same general pentacoordinate structure as found earlier for the $[Cu^{II}((imidH)_2DAP)]^{2+}$ parent compound, and it is assumed that $[Cu^{I}((5\text{-MeimidH})_2DAP)]^{+}$ is also pentacoordinate as is its Cu(I) parent compound. The present temperature-dependent electron self-exchange data are some of the first such data to be obtained for a synthetic Cu(I/II) couple that remains coordination-number-invariant (CN = 5) during electron transfer. The present electron self-exchange rate constant, together with those for two other, related coodination-number-invariant Cu(I/II) couples ($[Cu^{I,II}((imidH)_2DAP)]^{+/2+}$ and $[Cu^{I,II}((py)_2DAP)]^{+/2+}$) indicate a possible relationship between intramolecular conformational mobility in the Cu(I) partner complex and the electron self-exchange rate of the Cu(I/II) couple. Because of its coordination-number invariance, this small-molecule system resembles the situation at the active site in the blue copper protein plastocyanin (CN = 4) and possibly azurin. It is noteworthy that azurin has a much greater ΔH^* for electron exchange than does the present synthetic system. Crystal data for $[Cu^{II}((5\text{-MeimidH})_2DAP)](BF_4)_2 \cdot {}^1/_2CH_3OH$, $CuF_8O_{0.5}N_7B_2C_{21.5}H_{29}$: a = 11.983 (4) Å, b = 10.360 (4) Å, c = 12.906 (6) Å, α = 68.51 (3)°, β = 73.63 (3)°, γ = 67.06 (3)°, Z = 2, triclinic, space group $P\bar{1}$. A total of 7592 observed data were collected at −155 ± 5 °C and used in the solution. The pentacoordinate cation is disordered into two enantiometric forms around the copper(II) ion. The structures are closer to idealized trigonal bipyramidal than square pyramidal. Crystal data for $[Cu^{II}((imidH)_2DAP)](BF_4)_2$, $CuF_8N_7B_2C_{19}H_{23}$: a = 12.431 (9) Å, b = 14.024 (6) Å, c = 14.296 (11) Å, β = 104.45 (6)°, Z = 4, monoclinic, space group $P2_1/c$. A total of 1358 observed data were obtained. The structure of the cation (as its BF_4^- salt) is more square pyramidal than that of the perchlorate salt whose structure had been previously determined.

Introduction

Unlike heme iron and iron–sulfur electron-transfer proteins, cuproproteins have no extrudable coordination complex, since the active-site structure exists only through chelation of the copper ion with protein residues.[5] Therefore, the study of small-molecule copper complexes (i.e., model compounds) provides one of the only means by which the active-site contribution to electron transfer can be evaluated. For plastocyanin of the blue copper family of electron-transfer proteins, modeling of the active site requires a retained geometry and coordination number (CN = 4) about the metal center during electron transfer and the assurance of an outer-sphere mechanism. Such restrictions are not trivially accommodated in designing synthetic systems for study, since copper is known for its high kinetic lability and its tendency to adopt different coordination geometries and numbers in the +1 and +2 oxidation states. Additionally, an ideal model compound ligand for plastocyanin would present an (N_2SS^*) donor atom set similar to that observed at the active site of the protein. The most common approach toward modeling blue copper active sites has been the design of multidentate ligands with S and N donor atoms,[6-13] but

(1) Taken in part from: Coggin, D. K. Ph.D. Dissertation, Rice University, 1990.
(2) Rice University.
(3) University of Notre Dame.
(4) Auburn University.
(5) Solomon, E. I. In *Copper Coordination Chemistry: Biochemical & Inorganic Perspectives*; Karlin, K. D.; Zubieta, J., Eds.; Adenine Press: Guilderland, NY, 1983; pp 1-22.
(6) Goodwin, J. A.; Stanbury, D. M.; Wilson, L. J.; Eigenbrot, C. W.; Scheidt, W. R. *J. Am. Chem. Soc.* **1987**, *109*, 2979-2991.
(7) Goodwin, J. A.; Bodager, G. A.; Wilson, L. J.; Stanbury, D. M.; Scheidt, W. R. *Inorg. Chem.* **1989**, *28*, 35-42.
(8) Goodwin, J. A.; Wilson, L. J.; Stanbury, D. M.; Scott, R. A. *Inorg. Chem.* **1989**, *28*, 42-50.
(9) Korp, J. D.; Bernal, I.; Merrill, C. L.; Wilson, L. J. *J. Chem. Soc., Dalton Trans.* **1981**, 1951-1956.
(10) Martin, M. J.; Endicott, J. F.; Ochrymowycz, L. A.; Rorabacher, D. B. *Inorg. Chem.* **1987**, *26*, 3012-3022.

0020-1669/91/1330-1125$02.50/0

an unfortunate characteristic of these synthetic Cu(I/II) redox couples has been the tendency to have an increase in the coordination number of the Cu(II) derivative relative to that of the Cu(I) species.[14-19]

Only rarely have synthetic, coordination-number-invariant copper(I/II) couples been encountered that could serve as useful model compounds for the active-site situation in blue copper proteins. Of these, the $[Cu^{I,II}((imidH)_2DAP)]^{+/2+}$ couple, which has in both oxidation states the structure

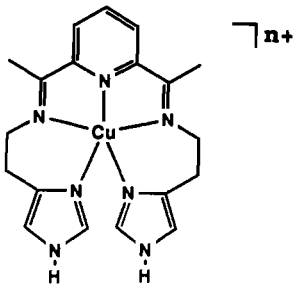

and its close structural relatives have been shown to exhibit pentacoordinate structures for Cu(I) and Cu(II) in both the solid and solution states.[6,7] Although the $[CuN_5]^{+/2+}$ core of these structures does not exactly mimic the $[CuN_2SS^*]^{0/+}$ core of plastocyanin, both the synthetic[6-8] and the naturally occurring[20,21] copper centers are coordination number invariant under redox turnover, and both are belived to undergo electron transfer by an outer-sphere mechanism.[20,21] With such strong parallels between this synthetic system and the naturally occurring copper system of interest, we have initiated a program of study, aimed at a more thorough understanding of copper electron-transfer reactions, by scrutinizing the redox chemistry of the $[Cu^{I,II}((imidH)_2DAP)]^{+/2+}$ cations and their close structural analogues.

The electron self-exchange rates for a number of small-molecule Cu(I/II) redox couples have been estimated by applying Marcus theory to cross-exchange rate data.[6,10,11,22] Most studies of the cross-exchange kinetics of copper complexes have involved the reduction of the Cu(II) species. For some cases where the oxidation reactions have been compared with the corresponding reduction reactions, the Marcus cross-relationship has yielded different values for the self-exchange rate constant, k_{ex}, of a given Cu(I/II) couple.[10,22] Martin et al. have proposed that the deviations from Marcus behavior for some copper–polythia ether complexes may be due to a dual-pathway (square) mechanism in which conformational reorganization and electron transfer are sequential rather than concerted.[10] On the other hand, Lee and

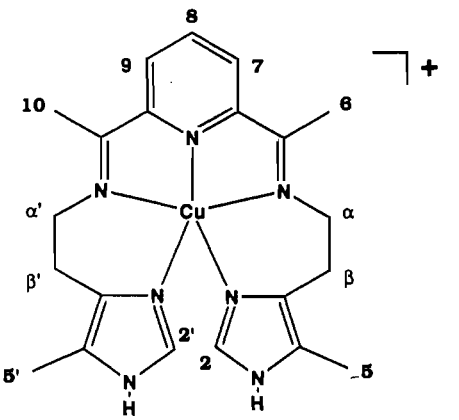

Figure 1. Schematic representation of the $[Cu^{I}((5\text{-}MeimidH)_2DAP)]^{+}$ cation with the proton-labeling scheme.

Anson have suggested that the discordant k_{ex} values of some copper–polypyridyl complexes are due to the fact that the Cu(II) and Cu(I) species do not contribute equally to the activation barrier.[23] These findings suggest a need for direct determination of electron self-exchange rates of well-conceived, small-molecule Cu(I/II) couples if a model compound approach is to be constructively employed in probing active-site contributions to cuproprotein electron transfer. In this connection, it also seems essential to demonstrate coordination number invariance by using various structural techniques such as crystallography and EXAFS.

To date, experimentally determined Cu(I) ⇄ Cu(II) self-exchange rate constants have been reported for (i) $[Cu(phen)_2]^{+/2+}$ (phen = 1,10-phenanthroline) at a graphite electrode in aqueous chloride media,[24] (ii) $[Cu(dmp)_2]^{+/2+}$ (dmp = 2,9-dimethyl-1,10-phenanthroline) in D_2O, CD_3CN, and acetone-d_6,[25] (iii) $[Cu(TAAB)]^{+/2+}$ (TAAB = tetrabenzo[*b,f,j,n*][1,5,9,13]tetraazacyclohexadecine) in methanol-d_4,[12] (iv) $[Cu(bidhp)]^{+/2+}$ (bidhp = 1,7-bis(5-methylimidazole-4-yl)-1,6-dithiaheptane) in DMSO-d_6,[13] (v) $[Cu((py)_2DAP)]^{+/2+}$ ($(py)_2DAP$ = 2,6-bis[1-((2-pyridin-2-ylethyl)imino)ethyl]pyridine) in CD_3CN[6] (vi) $[Cu((imidH)_2DAP)]^{+/2+}$ ($(imidH)_2DAP$ = 2,6-bis[1-((2-imidazol-4-ylethyl)imino)ethyl]pyridine) in CD_3CN,[8] and (vii) three macrocyclic N,S complexes in aqueous solution.[26] Moreover, Knapp et al.[27] have reported an *upper* limit for a pseudotetrahedral system. Presented here is the direct measurement of the self-exchange electron-transfer rate, as a function of temperature, in CD_3CN for the $[Cu^{I,II}((5\text{-}MeimidH)_2DAP)]^{+/2+}$ couple by dynamic NMR techniques. This new pentadentate ligand, the 5-methylimidazole-substituted derivative of $(imidH)_2DAP$, has been designed to prevent an undesirable side reaction (ligand cyclization) that has been observed for the $(imidH)_2DAP$ parent complex.[7] In addition, conformational mobility in three $[Cu^{I}((arm)_2DAP)]^{+}$ complexes (where (arm) = py, imidH, and 5-MeimidH) has been reported in the preceding paper.[28] The results provide the first insight into a possible connection between rates of ligand fluctionality in the Cu(I) comlexes and the rates of electron self-exchange for the Cu(I/II) couples. Also reported in this work are two X-ray crystal structures: one is of the new, pentacoordinate $[Cu^{II}((5\text{-}MeimidH)_2DAP)](BF_4)_2$ complex, and the other is of $[Cu^{II}((imidH)_2DAP)](BF_4)_2$. The latter has already been reported as the ClO_4^- salt,[9] and taken together, the two demonstrate a significant influence of crystal packing forces on the coordination geometry.

(11) Karlin, K. D.; Yandell, J. K. *Inorg. Chem.* **1984**, *23*, 1184–1188.
(12) Pulliam, E. J.; McMillin, D. R. *Inorg. Chem.* **1984**, *23*, 1172–1175.
(13) Groeneveld, C. M.; van Rijn, J.; Canters, G. W. *J. Am. Chem. Soc.* **1988**, *110*, 4893–4900.
(14) Rorabacher, D. B.; Martin, M. J.; Koenigbauer, M. J.; Malik, M.; Schroeder, R. R.; Endicott, J. F.; Ochrymowycz, L. A. In *Copper Coordination Chemistry: Biochemical & Inorganic Perspectives*; Karlin, K. D., Zubieta, J., Eds.; Adenine Press: Guilderland, NY, 1983; pp 167–202.
(15) Zubieta, J.; Karlin, K. D.; Hayes, J. C. In *Copper Coordination Chemistry: Biochemical & Inorganic Perspectives*; Karlin, K. D., Zubieta, J., Eds.; Adenine Press: Guilderland, NY, 1983; pp 97–108.
(16) Brubaker, G. R.; Brown, J. N.; Yoo, M. K.; Kinsey, R. A.; Kutchan, T. M. *Inorg. Chem.* **1979**, *18*, 299–302.
(17) van Rijn, J.; Driessen, W. L.; Reedijk, J.; Lehn, J.-M. *Inorg. Chem.* **1984**, *23*, 3584–3588.
(18) Reedijk, J.; Driessen, W. L.; van Rijn, J. In *Biological and Inorganic Copper Chemistry*, Karlin, K. D., Zubieta, J., Eds.; Adenine Press: Guilderland, NY, 1985, Vol. 2, pp 143–160.
(19) Birker, P. J. M. W. L.; Reedijk, J. In *Copper Coordination Chemistry: Biochemical & Inorganic Perspectives*: Karlin, K. D., Zubieta, J., Eds.; Adenine Press: Guilderland, NY, 1983; pp 409–424.
(20) Armstrong, F. A.; Driscoll, P. C.; Hill, H. A. O. *FEBS Lett.* **1985**, *190*, 242–248.
(21) Guss, J. M.; Harrowell, P. R.; Murata, M.; Norris, V. A.; Freeman, H. C. *J. Mol. Biol.* **1986**, *192*, 361–387.
(22) Yandell, J. K. In *Copper Coordination Chemistry: Biochemical and Inorganic Perspectives*; Karlin, K. D.; Zubieta, J., Eds.; Adenine Press: Guilderland, NY, 1983, pp 157–166.
(23) Lee, C.-W.; Anson, F. C. *J. Phys. CHem.* **1983**, *87*, 3360–3362.
(24) Lee, C.-W.; Anson, F. C. *Inorg. Chem.* **1984**, *23*, 837–844.
(25) Doine, H.; Yano, Y.; Swaddle, T. W. *Inorg. Chem.* **1989**, *28*, 2319–2322.
(26) Rorabacher, D. B.; Bernardo, M. M.; Vande Linde, A. M. Q.; Leggett, G. H.; Westerby, B. C.; Martin, M. J.; Ochrymowycz, L. A. *Pure Appl. Chem.* **1988**, *60*, 501–508.
(27) Knapp, S.; Keenan, T. P.; Zhang, X.; Fikar, R.; Potenza, J. A.; Schugar, H. J. *J. Am. Chem. Soc.* **1990**, *112*, 3452–3464.
(28) Coggin, D. K.; González, J. A.; Kook, A. M.; Stanbury, D. M.; Wilson, L. J. *Inorg. Chem.*, preceding paper in this issue.

Experimental Section

$[Cu^{II}((5\text{-MeimidH})_2DAP)](BF_4)_2$. This compound was prepared by the general method of Simmons et al.[29] and purified by low-pressure column chromatography as reported in the preceding paper.[28] A single-crystal X-ray structure of the $[Cu^{II}((5\text{-MeimidH})_2DAP)](BF_4)_2 \cdot {}^1/_2CH_3OH$ compound is presented below.

$[Cu^{I}((5\text{-MeimidH})_2DAP)](BF_4)$. This compound was prepared and isolated as the CH_2Cl_2 solvate by the general method of Goodwin et al.,[6,8] as reported in the preceding paper.[28] Because $[Cu^{I}((5\text{-MeimidH})_2DAP)](BF_4)$ in solution is easily oxidized by O_2, the compound was always handled anaerobically.

NMR Measurements. Proton NMR spectra were recorded at 300 MHz on an IBM/Bruker AF-300 NMR spectrometer. Samples of $[Cu^{I}((5\text{-MeimidH})_2DAP)](BF_4)$ (10 mM) in deoxygenated CD_3CN, with varying concentrations of $[Cu^{II}((5\text{-MeimidH})_2DAP)](BF_4)_2$ and Me_4NBF_4 for μ = 25 mM, were prepared in the drybox from the solid Cu(I) salt. Sample preparation proceeded as follows: a 3 mL CD_3CN stock solution 10 mM in Cu(I) was prepared in a volumetric flask. Solutions A (2 mL; 10 mM in $[Cu^{I}((5\text{-MeimidH})_2DAP)](BF_4)$ and 15 mM in Me_4NBF_4) and B (0.5 mL; 10 mM in $[Cu^{I}((5\text{-MeimidH})_2DAP)](BF_4)$ and 5 mM in $[Cu^{II}((5\text{-MeimidH})_2DAP)](BF_4)_2$) were subsequently prepared from the stock solution. The NMR samples were then prepared by mixing the appropriate volumes of solutions A and B in an NMR tube. The 5-mm tubes (Wilmad, precision grade) were well sealed with a rubber septum and Parafilm.

NMR spectra were obtained at various temperatures between 243 and 293 K. Typically, a FID consisted of 128, 32 K scans. The frequency-domain NMR data of the H 2,2′ resonance (as indicated in Figure 1) were fit by a Lorentzian line shape by using DISP, the line-shape program available on the IBM/Bruker spectrometer. T_2^{-1} values were obtained by multiplying the line widths at half-height ($\Delta\nu_{1/2}$) by π. Acetonitrile-d_3 (Aldrich, 99 atom % D) used in the T_2^{-1} measurements was deoxygenated by the freeze–pump–thaw method. The chemical shift of the CH_3CN-d_2 signal served as an internal standard and was set to 1.93 ppm.

Second-order rate constants and activation parameters were obtained by fitting the $1/T_2$ values with the appropriate equations, using the Los Alamos non-linear least-squares computer program. The data were weighted proportionally to T_2^2. Uncertainties cited represent 1 standard deviation.

Crystal Growth. Crystals of $[Cu^{II}((5\text{-MeimidH})_2DAP)](BF_4)_2 \cdot {}^1/_2CH_3OH$ and $[Cu^{II}(imidH)_2DAP)](BF_4)_2$[30] suitable for X-ray diffraction were grown under ambient conditions in the dark by vapor diffusion of anhydrous diethyl ether into dilute methanol solutions of their respective salts.

X-ray Data Collection. $[Cu^{II}((5\text{-MeimidH})_2DAP)](BF_4)_2 \cdot {}^1/_2CH_3OH$. Initial attempts to collect diffraction data at ambient conditions were unsuccessful owing to apparent crystal decomposition, and accordingly, all subsequent diffraction measurements were performed at low temperature (−155 ± 5 °C). A dark green, irregularly shaped crystal with approximate dimensions of 0.95 × 0.40 × 0.40 mm³ was mounted on a glass fiber. The crystal, covered with a mixture of Paratone N and mother liquor, was quickly transferred to an Enraf-Nonius CAD4 diffractometer under a cold stream of nitrogen gas. Preliminary crystal examination and data collection were performed with graphite-monochromated Mo Kα radiation ($\bar{\lambda}$ = 0.71073 Å). The cell constants were obtained from a least-squares refinement of the setting angles of 25 reflections in the range $23 > 2\theta > 27°$.

Intensity data were collected by using θ–2θ scans to a 2θ of 65.3°. A total of 10350 reflections were collected. A total of 7592 reflections had $F_o^2 > 3\sigma(F_o^2)$ and were considered observed. The agreement of the 670 duplicate observed and averaged data was 1.6% on I and 1.4% on F_o. Before being averaged, the data were empirically corrected for the effect of absorption (μ = 8.87 cm⁻¹). Four representative reflections were measured every hour of X-ray exposure as a check on crystal stability. The slopes of the least-squares lines through plots of intensity versus time were −0.15, 0.00, 0.02, and −0.07%/h, which corresponds to an average total decay of 6.4% over 127.2 h of X-ray exposure. Due to the large variation among the four standards, no decay correction was applied. The crystal data and intensity collection parameters are summarized in Table I.

$[Cu^{II}((imidH)_2DAP)](BF_4)_2$. A blue-green rectangular column having approximate dimensions of 0.40 × 0.20 × 0.20 mm³ was mounted on a glass fiber with epoxy cement. All measurements were performed at room temperature (23 °C) on a Rigaku AFC5S diffractometer with graphite-monochromated Mo Kα radiation ($\bar{\lambda}$ = 0.71073 Å). The cell constants and orientation matrix for data collection were derived from a least-squares refinement of 25 carefully centered reflections in the range $4 < 2\theta < 12°$.

Intensity data were collected by using 2θ–ω scans to a 2θ of 55.1° [Rigaku CRYSTAN/TEXTL (4:0:0) automatic data collection series (Molecular Structure Corp.)].[31] A total of 5293 reflections were collected, 5036 of which were unique. The intensities of three representative reflections, which were measured every 150 reflections, decreased by an average of 0.6%. The data were corrected for absorption (φ-scan), decay, and Lorentz–polarization effects. A total of 1358 reflections with $I > 3.0\sigma(I)$ were used in the final refinement. The crystal data and intensity collection parameters are presented in Table I.

Table I. Summary of Crystal Data and Intensity Collection Parameters for $[Cu^{II}((5\text{-MeimidH})_2DAP)](BF_4)_2 \cdot {}^1/_2CH_3OH$ and $[Cu^{II}((imidH)_2DAP)](BF_4)_2$

	$[Cu^{II}((5\text{-MeimidH})_2DAP)](BF_4)_2 \cdot {}^1/_2CH_3OH$	$[Cu^{II}((imidH)_2DAP)](BF_4)_2$
T, °C	−155	23
formula	$C_{21.5}H_{29}N_7B_2F_8O_{0.5}Cu$	$C_{19}H_{23}N_7B_2F_8Cu$
fw, g	630.7	586.6
space group	$P\bar{1}$	$P2_1/c$
cryst syst	triclinic	monoclinic
a, Å	11.983 (4)	12.431 (9)
b, Å	10.360 (4)	14.024 (6)
c, Å	12.906 (6)	14.296 (11)
α, deg	68.51 (3)	
β, deg	73.63 (3)	104.45 (6)
γ, deg	67.06 (3)	
V, Å³	1354.8 (9)	2413 (3)
Z	2	4
d(calcd), g/cm³	1.50	1.61
radiation[a]	Mo Kα ($\bar{\lambda}$ = 0.71073 Å)	Mo Kα ($\bar{\lambda}$ = 0.71073 Å)
diffractometer	Enraf-Nonius CAD4	Rigaku AFC5S
scan technique	θ-2θ	2θ-ω
no. of unique obsd data	7592	1358
no. of variables	501	142
residuals	R_1 = 0.089	R_1 = 0.094
	R_2 = 0.139	R_2 = 0.108
data/param	15.2	9.6

[a] Graphite monochromated.

Crystal Structure Determinations. $[Cu^{II}((5\text{-MeimidH})_2DAP)](BF_4)_2 \cdot {}^1/_2CH_3OH$. The initial work was done by assuming the centrosymmetric space group $P\bar{1}$. The structure was partially solved using the direct methods program MULTAN78.[32] Difference Fourier syntheses phased by this partial solution showed that there was apparent disorder in the two attached imidazole arms of the pentadentate ligand. The disorder seemed to define the two possible enantiomorphs of the complex having idealized C_2 symmetry. Accordingly, the possibility that the correct space group was the noncentrosymmetric choice $P1$ was considered. The structure was redetermined in the noncentrosymmetric space group by using MULTAN78. This new solution led to the equivalent disorder found before. It was concluded that the significant disorder involved in the structure was intrinsic to the molecule itself and was not the consequence of the choice of space group. All subsequent aspects of the structure determination and least-squares refinement were therefore performed in the centrosymmetric space group $P\bar{1}$. The disorder model, which was developed by difference Fourier syntheses and was used in the final least-squares refinement, assumed equal occupation of the two sets of imidazole sidearms. One of the two BF_4^- anions was also found to be

(29) Simmons, M. G.; Merrill, C. L.; Wilson, L. J.; Bottomley, L. A.; Kadish, K. M. *J. Chem. Soc., Dalton Trans.* **1980**, 1827–1837.
(30) Merrill, C. L.; Wilson, L. J.; Thamann, T. J.; Loehr, T. M.; Ferris, N. S.; Woodruff, W. H. *J. Chem. Soc., Dalton Trans.* **1984**, 2207–2221.
(31) All calculations in this crystal structure study were performed by using the TEXSAN crystallographic software package of the Molecular Structure Corp.
(32) Programs used in these crystal structure studies included local modifications of Main, Hull, Lessinger, Germain, Declerq, and Woolfson's MULTAN78, Jacobson's ALLS, Zalkin's FORDAP, Busing and Levy's ORFFE and ORFLS and Johnson's ORTEP2. Atomic form factors were taken from the following: Cromer, D. T.; Waber, J. T *International Tables of X-ray Crystallography*; Kynoch: Birmingham, England, 1974, Vol. IV, Table 2.2B. Real and imaginary corrections for anomalous dispersion in the form factor of the copper atoms were taken from the following: Cromer, D. T. *International Tables of X-ray Crystallography*; Kynoch: Birmingham, England, 1974, Vol. IV, Table 2.3.1. Scattering factors for hydrogen were taken from the following: Stewart, R. F.; Davidson, E. E.; Simpson, W. T. *J. Chem. Phys.* **1965**, *42*, 3175–3187. All calculations were performed on a VAX 11/730 computer.

Table II. Fractional Coordinates for $[Cu^{II}((5\text{-MeimidH})_2DAP)](BF_4)_2 \cdot {}^1/_2CH_3OH$[a]

atom	x	y	z
Cu	0.77741 (5)	0.56157 (6)	0.26914 (4)
N(1)	0.9564 (7)	0.5542 (10)	0.2237 (7)
N(1′)	0.7641 (8)	0.4435 (11)	0.1788 (8)
N(3)	1.1355 (8)	0.5858 (10)	0.1910 (8)
N(3′)	0.6984 (9)	0.3217 (11)	0.1122 (9)
N(9)	0.8365 (4)	0.3628 (4)	0.3871 (3)
N(17)	0.6631 (4)	0.5958 (4)	0.4025 (3)
N(20)	0.6734 (4)	0.7697 (4)	0.2063 (3)
N(26)	0.6826 (9)	0.4592 (10)	0.0243 (7)
N(26′)	1.0725 (8)	0.7215 (11)	0.1217 (9)
N(28)	0.7513 (7)	0.5177 (10)	0.1355 (7)
N(28′)	0.9181 (7)	0.6362 (9)	0.1771 (7)
C(2)	1.0141 (16)	0.6505 (19)	0.2083 (15)
C(2′)	0.6725 (12)	0.4499 (13)	0.1334 (10)
C(4)	1.1599 (9)	0.4424 (11)	0.2066 (9)
C(4′)	0.8050 (13)	0.2325 (12)	0.1483 (10)
C(5)	1.2875 (13)	0.3317 (15)	0.2020 (13)
C(5′)	0.8549 (14)	0.0850 (17)	0.1311 (13)
C(6)	1.0488 (8)	0.4204 (11)	0.2241 (9)
C(6′)	0.8480 (10)	0.3068 (11)	0.1860 (8)
C(7)	1.0205 (10)	0.2866 (10)	0.2465 (8)
C(7′)	0.9648 (11)	0.2641 (13)	0.2299 (9)
C(8)	0.9412 (5)	0.2409 (6)	0.3651 (4)
C(10)	0.7736 (5)	0.3552 (6)	0.4855 (4)
C(11)	0.7995 (6)	0.2220 (7)	0.5833 (5)
C(12)	0.6723 (5)	0.4902 (6)	0.4988 (4)
C(13)	0.5920 (6)	0.5118 (7)	0.5965 (5)
C(14)	0.5038 (7)	0.6512 (8)	0.5898 (5)
C(15)	0.4983 (5)	0.7607 (6)	0.4884 (4)
C(16)	0.5802 (4)	0.7298 (5)	0.3945 (4)
C(18)	0.5896 (4)	0.8291 (5)	0.2771 (4)
C(19)	0.5027 (5)	0.9828 (6)	0.2532 (5)
C(21)	0.6896 (5)	0.8554 (6)	0.0858 (4)
C(22)	0.7938 (5)	0.7642 (7)	0.0174 (4)
C(23)	0.7493 (9)	0.6233 (10)	0.0320 (8)
C(23′)	0.9064 (8)	0.7379 (10)	0.0684 (8)
C(24)	0.7115 (10)	0.5907 (13)	−0.0381 (8)
C(24′)	1.0028 (8)	0.7918 (11)	0.0328 (9)
C(25)	0.6972 (13)	0.6614 (15)	−0.1571 (13)
C(25′)	1.0388 (10)	0.8958 (12)	−0.0740 (9)
C(27)	0.7103 (12)	0.4224 (13)	0.1274 (10)
C(27′)	1.0159 (15)	0.6333 (18)	0.1986 (14)
B(29)	−0.3631 (6)	0.2344 (7)	−0.1025 (5)
B(34)	0.2123 (13)	0.1134 (19)	−0.4606 (15)
B(34′)	0.2146 (13)	0.0390 (16)	−0.3893 (13)
OC(39)	0.0366 (27)	0.4508 (23)	−0.4925 (21)
OC(40)	−0.0641 (28)	0.430 (5)	−0.4435 (25)
OC(41)	−0.1318 (20)	0.589 (3)	−0.4285 (18)
F(30)	−0.4253 (4)	0.2062 (6)	−0.1596 (4)
F(31)	−0.3658 (6)	0.3802 (5)	−0.1508 (4)
F(32)	−0.4191 (4)	0.2220 (4)	0.00857 (29)
F(33)	−0.2448 (4)	0.1492 (6)	−0.1077 (4)
F(35)	0.2358 (10)	0.0645 (11)	−0.5457 (10)
F(35′)	0.2687 (8)	−0.1133 (10)	−0.3412 (7)
F(36)	0.3066 (11)	0.0435 (23)	−0.4073 (16)
F(36′)	0.305 (3)	0.070 (4)	−0.455 (6)
F(37)	0.2051 (14)	0.2530 (18)	−0.4895 (18)
F(37′)	0.1994 (17)	0.1020 (20)	−0.3090 (22)
F(38)	0.0996 (14)	0.0943 (24)	−0.3946 (22)
F(38′)	0.1235 (25)	0.0611 (26)	−0.4255 (29)

[a] The estimated standard deviations of the least significant digits are given in parentheses.

disordered, as was the half-molecule of methanol. The methanol molecule was found near the inversion center at 0, ${}^1/_2$, $-{}^1/_2$ and was described as three positions each at one-third occupancy and with the average O, C scattering factor. All atomic positions that were separated by more than 0.5 Å in the disorder model were refined as anisotropic atoms. The two distinct orientations of the imidazole arms were designated with primed and nonprimed atomic labels. The final model had 501 refined variables and 7952 observed data to give a final data/parameter ratio of 15.2; the final agreement factors were $R_1 = 0.089$ and $R_2 = 0.139$.[33] The atomic coordinates are listed in Table II.

(33) $R_1 = \sum||F_o| - |F_c||/\sum|F_o|$ and $R_2 = [\sum(|F_o| - |F_c|)^2/\sum w(F_o)^2]^{1/2}$.

Table III. Fractional Coordinates for $[Cu^{II}((imidH)_2DAP)](BF_4)_2$

atom	x	y	z
Cu	0.2786 (2)	0.8469 (1)	0.3007 (2)
N(1)	0.220 (1)	0.722 (1)	0.244 (1)
C(2)	0.205 (2)	0.641 (1)	0.292 (1)
N(3)	0.151 (1)	0.584 (1)	0.219 (1)
C(4)	0.132 (2)	0.623 (1)	0.132 (1)
C(5)	0.178 (2)	0.710 (1)	0.149 (1)
C(6)	0.181 (2)	0.788 (1)	0.082 (1)
C(7)	0.121 (2)	0.879 (1)	0.100 (1)
N(8)	0.173 (1)	0.921 (1)	0.192 (1)
C(9)	0.150 (1)	1.004 (1)	0.217 (1)
C(10)	0.074 (2)	1.069 (1)	0.149 (2)
C(11)	0.197 (2)	1.028 (1)	0.314 (1)
C(12)	0.181 (2)	1.118 (1)	0.363 (2)
C(13)	0.226 (2)	1.123 (2)	0.457 (2)
C(14)	0.290 (2)	1.052 (2)	0.509 (2)
C(15)	0.308 (2)	0.970 (1)	0.461 (1)
N(16)	0.264 (1)	0.963 (1)	0.369 (1)
C(17)	0.378 (2)	0.885 (1)	0.498 (1)
C(18)	0.447 (2)	0.889 (2)	0.603 (2)
N(19)	0.377 (1)	0.820 (1)	0.439 (1)
C(20)	0.455 (2)	0.738 (1)	0.463 (2)
C(21)	0.481 (2)	0.699 (1)	0.377 (2)
C(22)	0.510 (2)	0.772 (1)	0.310 (1)
C(23)	0.610 (2)	0.783 (2)	0.288 (2)
N(24)	0.595 (1)	0.855 (1)	0.227 (1)
C(25)	0.491 (2)	0.894 (1)	0.210 (1)
N(26)	0.441 (1)	0.841 (1)	0.266 (1)

$[Cu^{II}((imidH)_2DAP)](BF_4)_2$. The present structure was solved by using the direct methods programs MITHRIL[34] and DIRDIF[35] to locate the Cu atoms and non-hydrogen atoms, respectively. Anisotropic temperature factors were assigned to the Cu atoms only. All remaining atoms were refined isotropically. Because the BF_4^- anions were found to be disordered, they were treated as rigid groups; the ratios of the occupancies for the B and F atoms were set to 50/50 for one BF_4^- ion and 49/51 for the other ion. Hydrogen atoms were included in the structure factor calculation in idealized positions (C–H = 0.95 Å). Their assigned isotropic thermal parameters were 20% greater than the B(eq) value for the atom to which they were bonded. The final model (based on 1358 observed reflections and 142 variable parameters) converged with agreement factors of $R_1 = 0.094$ and $R_2 = 0.108$.[33] Final values of the atomic coordinates are listed in Table III.

Results

Electron Self-Exchange Measurements. The electron self-exchange rate constant, k'_{44} (M^{-1} s^{-1}), for the $[Cu^{I/II}((5\text{-MeimidH})_2DAP)]^{+/2+}$ couple was measured by using the line-width ($\Delta\nu_{1/2}$) method for the determination of $1/T_2$. The notation k'_{44} is used to be consistent with our prior studies: the prime mark designates that the rate constant has not been corrected for activity coefficients or ion pairing; the subscript 44 designates the identity of the complex. The exchange rate is related to $1/T_{2obs}$ according to

$$\pi\Delta\nu_{1/2} = 1/T_{2obs} = 1/T_{2n} + 1/T_{2e} = 1/T_{2n} + k_{ex}[P] \qquad (1)$$

which is valid in the slow-exchange regime.[13,36] In this equation, T_{2n} is the natural transverse relaxation time of the diamagnetic species in the absence of exchange, T_{2e} is the contribution to the observed transverse relaxation time (T_{2obs}) due to chemical exchange, and [P] is the concentration of the paramagnetic species. A plot of $1/T_{2obs}$ versus [P] gives a straight line with a slope equal to the exchange rate constant, which is k'_{44} in the present case. Since an NMR spectrum of $[Cu^{II}((5\text{-MeimidH})_2DAP)]^{2+}$ is unobservable because of paramagnetic broadening, the spectra of the mixed samples show the resonance of the Cu(I) species only. $[Cu^{I}((5\text{-MeimidH})_2DAP)]^{+}$ exhibits only one free-lying singlet suitable for line-broadening measurements: the 2,2′-proton res-

(34) Gilmore, C. J. *J. Appl. Cryst.* **1984**, *17*, 42–46.
(35) Beurskens, P. T.; DIRDIF Technical Report 1984/1; Crystallography Laboratory, Toernooiveld, 6525 Ed Nijmegen, Netherlands.
(36) Drago, R. S. *Physical Methods in Chemistry*; W. B. Saunders: Philadelphia, PA, 1977; pp 252–257.

Table IV. Variation of $1/T_2$ (Hz)[a] with the Concentration of Cu(II) in the $[Cu^{I/II}((5\text{-MeimidH})_2DAP)]^{+/2+}$ System[b] as a Function of Temperature

	$1/T_2$ for various concn of Cu(II)					
T, K	0.00 mM	0.20 mM	0.40 mM	0.60 mM	0.80 mM	k'_{44},[c] M^{-1} s^{-1}
293	19.85	21.32	31.57	40.43	48.95	3.53 (0.61) × 10^4
283	15.72	18.31	24.13	26.95	32.01	2.02 (0.15) × 10^4
273	12.16	13.08	19.10	24.60	26.86	1.95 (0.32) × 10^4
263	10.90	12.97	14.17	20.55	21.39	1.33 (0.23) × 10^4
253	10.04	11.28	12.57	17.53	21.21	1.25 (0.26) × 10^4
243	10.10	11.03	12.28	14.17	17.40	8.1 (1.3) × 10^3

[a] From the line width $\Delta\nu_{1/2}$ of the 2,2'-proton resonance of $[Cu^I((5\text{-MeimidH})_2DAP)]^+$ (Figure 1). [b] In acetonitrile-d_3 with [Cu(I)] = 10 mM, μ = 25 mM (Me_4NBF_4). [c] Derived from the least-squares fit of $1/T_{2,exp}$ (Hz) vs [Cu(II)] plots; standard deviations are given in parentheses.

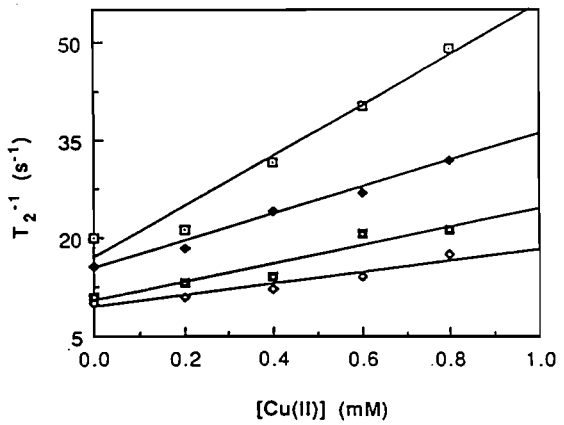

Figure 2. Plot of T_2^{-1} (s^{-1}) versus $[[Cu^{II}((5\text{-MeimidH})_2DAP)]^{2+}]$ (mM) for the 2,2'-proton resonance of $[Cu^I((5\text{-MeimidH})_2DAP)]^+$ at various temperatures: (⊡) 293 K, (◆) 283 K, (□) 263 K, (◇) 243 K. Measurements were performed with $[Cu^I((5\text{-MeimidH})_2DAP)]^+$ at 10 mM and μ = 25 mM (Me_4NBF_4).

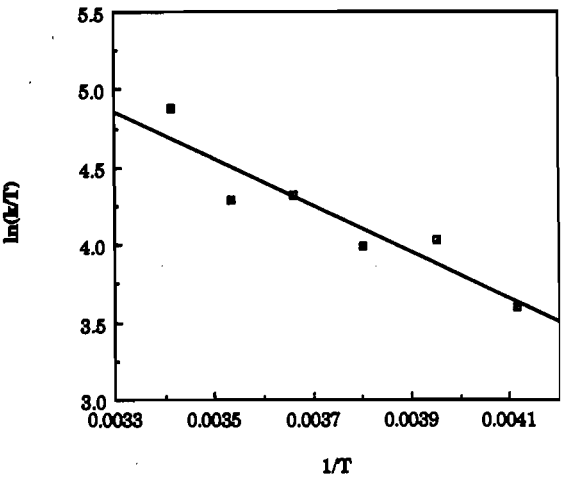

Figure 3. Eyring plot of the rate data for the electron self-exchange reaction of $[Cu((5\text{-MeimidH})_2DAP)]^{+/2+}$ in CD_3CN, μ = 25 mM (Me_4NBF_4).

onance at δ = 7.34 (see Figure 1). The complete ^1H NMR spectrum of the compound is given elsewhere.[28] T_2^{-1} measurements were obtained at six different temperatures to determine the exchange regime of the 2,2'-proton resonance. The slow-exchange limit applies when an increase in temperature produces an increase in k'_{44}.[13] Values of $1/T_2$ are listed in Table IV, and plots of $1/T_2$ vs added $[Cu^{II}((5\text{-MeimidH})_2DAP)]^{2+}$ are illustrated in Figure 2; for purposes of clarity, only four of the six temperatures are shown. A least-squares analysis of the data yielded the values of k'_{44} summarized in Table IV. The experimental value for k'_{44} is 3.53 × 10^4 M^{-1} s^{-1} at μ = 0.025 M and T = 293 K,

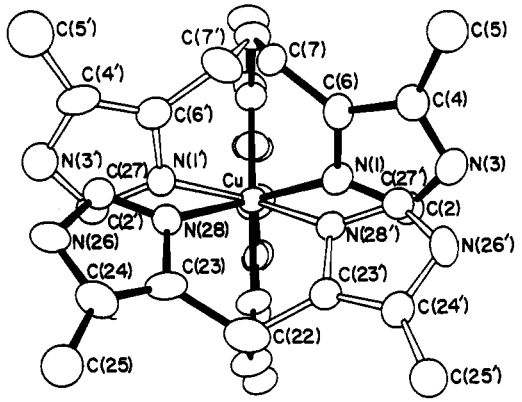

Figure 4. Drawing of the disorder model used in the final least-squares refinement. A view of the two disordered orientations of the $[Cu^{II}((5\text{-MeimidH})_2DAP)]^{2+}$ cation as viewed down the pseudo-2-fold axis.

Table V. Selected Bond Distances (Å) in $[Cu^{II}((5\text{-MeimidH})_2DAP)](BF_4)_2 \cdot {}^1/_2CH_3OH$[a]

Cu–N(1)	2.036 (8)	N(28)–C(27)	1.308 (14)
Cu–N(1')	2.045 (9)	N(28')–C(23')	1.418 (12)
Cu–N(9)	2.058 (4)	N(28')–C(27')	1.264 (18)
Cu–N(17)	1.924 (4)	C(4)–C(5)	1.513 (17)
Cu–N(20)	2.013 (4)	C(4)–C(6)	1.380 (13)
Cu–N(28)	2.066 (8)	C(4')–C(5')	1.484 (18)
Cu–N(28')	2.017 (8)	C(4')–C(6')	1.348 (6)
N(1)–C(2)	1.352 (19)	C(6)–C(7)	1.462 (13)
N(1)–C(6)	1.396 (13)	C(6')–C(7')	1.502 (16)
N(1')–C(2')	1.353 (14)	C(7)–C(8)	1.572 (11)
N(1')–C(6')	1.368 (14)	C(7')–C(8)	1.627 (12)
N(3)–C(2)	1.336 (19)	C(10)–C(11)	1.485 (8)
N(3)–C(4)	1.344 (14)	C(10)–C(12)	1.481 (8)
N(3')–C(2')	1.354 (15)	C(12)–C(13)	1.386 (8)
N(3')–C(4')	1.343 (16)	C(13)–C(14)	1.407 (10)
N(9)–C(8)	1.441 (7)	C(14)–C(15)	1.380 (8)
N(9)–C(10)	1.273 (7)	C(15)–C(16)	1.379 (7)
N(17)–C(12)	1.320 (6)	C(16)–C(18)	1.490 (7)
N(17)–C(16)	1.343 (6)	C(18)–C(19)	1.498 (7)
N(20)–C(18)	1.279 (6)	C(21)–C(22)	1.516 (8)
N(20)–C(21)	1.482 (6)	C(22)–C(23)	1.673 (12)
N(26)–C(24)	1.425 (15)	C(22)–C(23')	1.553 (11)
N(26)–C(27)	1.344 (14)	C(23)–C(24)	1.308 (15)
N(26')–C(24')	1.413 (14)	C(23')–C(24')	1.369 (12)
N(26')–C(27')	1.311 (19)	C(24)–C(25)	1.468 (18)
N(28)–C(23)	1.382 (13)	C(24')–C(25')	1.478 (14)
B(29)–F(31)	1.398 (8)	B(29)–F(30)	1.350 (7)
B(29)–F(32)	1.382 (7)	B(34)–F(38)	1.424 (24)
B(29)–F(33)	1.345 (8)	B(34')–F(35')	1.416 (18)
B(34)–F(35)	1.291 (17)	B(34')–F(36')	1.250 (34)
B(34)–F(36)	1.308 (20)	B(34')–F(37')	1.352 (19)
B(34)–F(37)	1.328 (23)	B(34')–F(38')	1.215 (30)

[a] Estimated standard deviations in the least significant figure are given in parentheses.

and from the observed decrease in k'_{44} with decreasing temperature, the 2,2'-proton resonance is assumed to lie in the slow-exchange regime.

From the k'_{44} values in Table IV, the activation parameters of the electron-exchange reaction were determined by using the Eyring relationship[13]

$$k'_{44} = (kT/h)e^{-\Delta G^*/RT} = (kT/h)e^{-\Delta H^*/RT}e^{\Delta S^*/R} \quad (2)$$

in which k is the Boltzmann constant, h the Planck constant, R the gas constant, ΔG^* the free energy of activation, ΔH^* the activation enthalpy, and ΔS^* the activation entropy. The k'_{44} data have been used to construct the Eyring plot shown in Figure 3, and a least-squares analysis of the data points gives ΔH^* = 3.9 (0.8) kcal mol^{-1} or 16.2 (3.3) kJ mol^{-1} and ΔS^* = −24.6 (2.9) cal K^{-1} mol^{-1} or −103 (12) J K^{-1} mol^{-1}.

Crystal Structure Determinations. The disorder model for $[Cu^{II}((5\text{-MeimidH})_2DAP)]^{2+}$ used in the final least-squares refinement is illustrated in Figure 4; the primed and nonprimed

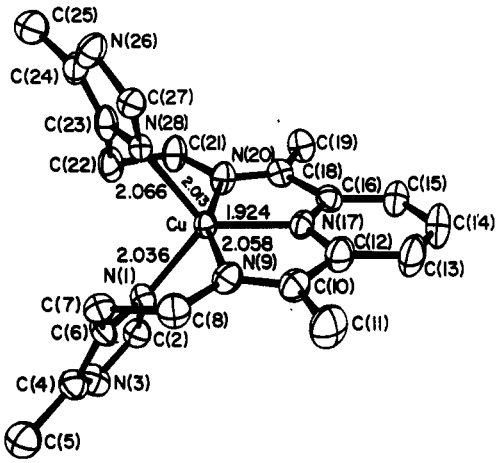

Figure 5. ORTEP drawing of the $[Cu^{II}((5\text{-MeimidH})_2DAP)]^{2+}$ cation with the atom-labeling scheme (nonprimed) and bond distances in the coordination group displayed. Ellipsoids are contoured at the 50% probability level.

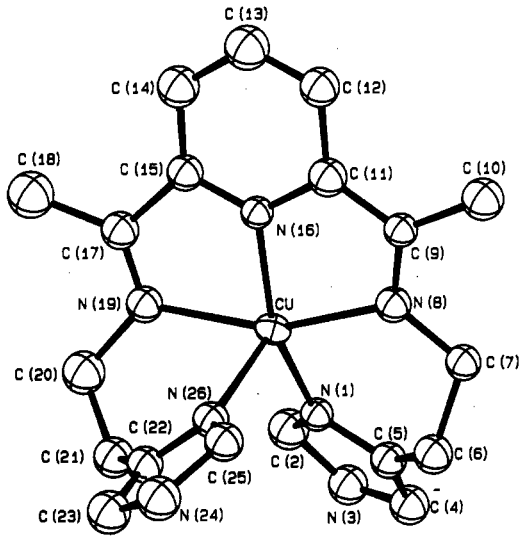

Figure 6. ORTEP drawing of the $[Cu^{II}((imidH)_2DAP)]^{2+}$ cation with the atom-labeling scheme. Ellipsoids are contoured at the 50% probability level.

orientations of the model are crystallographically independent and enantiomeric. The overall perspective view, as shown in Figure 5, illustrates the atom-labeling scheme and the Cu–N bond distances of one of the $[Cu^{II}((5\text{-MeimidH})_2DAP)]^{2+}$ cations. Selected bond distances are given in Table V, while the bond angles are listed in Table VI. This structure is clearly pentacoordinate about the Cu(II) ion, and the inner-sphere geometry may be best described as intermediate between a trigonal bipyramid and a square pyramid, based on the ideal values of the internal angles.

The overall perspective view of the $[Cu^{II}((imidH)_2DAP)]^{2+}$ cation, as shown in Figure 6, illustrates the atom-labeling scheme. Selected bond distances are listed in Table VII and bond angles are given in Table VIII. A previous structure determination of this cation had ClO_4^- as the counterion, whereas in the present study BF_4^- serves as the anion. Note that the two salts crystallize in different space groups. The geometry about the pentacoordinate Cu(II) center may be best described as a distorted square pyramid, as judged by the Cu–N bond distances and the values of the internal angles.

Discussion

Solid-State Structural Comparisons. Crystal structures of the $[Cu^{I/II}((imidH)_2DAP)]^{+/2+}$ and $[Cu^{I/II}((py)_2DAP)]^{+/2+}$ cations have been reported previously.[6,7,9] These structures share several features with the present $[Cu^{II}((5\text{-MeimidH})_2DAP)]^{2+}$ complex such as coordination number, molecular configuration, and ring conformation. The interrelationship between *configuration* (molecular helicity, i.e., Λ and Δ) and *conformation* (ring helicity, i.e., λ and δ) for these complexes is discussed in the preceding paper.[28] The three pentadentate ligands, $((imidH)_2DAP)$, $((5\text{-MeimidH})_2DAP)$, and $((py)_2DAP)$ differing only in their terminal imidazole (imidH), 5-methylimidazole (5-MeimidH), and pyridine (py) moieties), envelop the Cu(I/II) ions in the same general

Table VI. Selected Bond Angles (deg) in $[Cu^{II}((5\text{-MeimidH})_2DAP)](BF_4)_2 \cdot {}^1/_2CH_3OH$[a]

N(1)–Cu–N(9)	86.7 (3)	C(12)–N(17)–C(16)	122.4 (4)
N(1′)–Cu–N(9)	85.7 (3)	C(18)–N(20)–C(21)	119.5 (4)
N(1)–Cu–N(17)	129.5 (3)	C(24)–N(26)–C(27)	105.8 (9)
N(1′)–Cu–N(17)	122.9 (3)	C(24′)–N(26′)–C(27′)	105.6 (10)
N(1)–Cu–N(20)	107.7 (3)	C(23)–N(28)–C(27)	106.1 (9)
N(1′)–Cu–N(20)	106.1 (3)	C(23′)–N(28′)–C(27′)	104.7 (10)
N(1)–Cu–N(28)	101.5 (3)	N(1)–C(2)–N(3)	109.7 (13)
N(1′)–Cu–N(28′)	103.8 (3)	N(1′)–C(2′)–N(3′)	109.8 (11)
N(9)–Cu–N(17)	78.7 (2)	N(3)–C(4)–C(5)	124.5 (9)
N(9)–Cu–N(20)	158.1 (2)	N(3′)–C(4′)–C(5′)	117.1 (11)
N(9)–Cu–N(28)	106.6 (3)	C(5)–C(4)–C(6)	128.5 (10)
N(9)–Cu–N(28′)	111.7 (3)	C(5′)–C(4′)–C(6′)	133.9 (12)
N(17)–Cu–N(20)	79.4 (2)	N(1)–C(6)–C(4)	107.6 (8)
N(17)–Cu–N(28)	128.9 (2)	N(1′)–C(6′)–C(4′)	108.5 (10)
N(17)–Cu–N(28′)	133.1 (3)	N(1)–C(6)–C(7)	121.7 (8)
N(20)–Cu–N(28)	87.0 (3)	N(1′)–C(6′)–C(7′)	120.0 (9)
N(20)–Cu–N(28′)	83.9 (3)	C(6)–C(7)–C(8)	114.3 (8)
C(2)–N(1)–C(6)	106.0 (10)	C(6)–C(7′)–C(8)	112.3 (8)
C(2′)–N(1′)–C(6′)	105.9 (9)	C(7)–C(8)–C(9)	111.6 (5)
C(2)–N(3)–C(4)	109.3 (10)	C(7′)–C(8)–C(9)	106.5 (5)
C(2′)–N(3′)–C(4′)	107.0 (10)	N(9)–C(10)–C(11)	123.3 (5)
C(8)–N(9)–C(10)	121.0 (4)	N(9)–C(10)–C(12)	115.9 (5)
C(11)–C(10)–C(12)	120.8 (5)	C(23)–C(24)–N(26)	106.0 (9)
C(10)–C(12)–C(13)	127.5 (5)	C(23′)–C(24′)–N(26′)	105.2 (8)
C(10)–C(12)–N(17)	111.7 (4)	C(25)–C(24)–N(26)	121.4 (10)
C(13)–C(12)–N(17)	120.8 (5)	C(25′)–C(24′)–N(26′)	123.1 (9)
C(12)–C(13)–C(14)	117.6 (5)	N(26)–C(27)–N(28)	111.4 (10)
C(13)–C(14)–C(15)	120.3 (5)	N(26′)–C(27′)–N(28′)	116.1 (14)
C(14)–C(15)–C(16)	118.6 (5)	F(30)–B(29)–F(31)	108.4 (5)
C(15)–C(16)–N(17)	120.3 (5)	F(30)–B(29)–F(32)	111.6 (5)
C(15)–C(16)–C(18)	127.9 (5)	F(30)–B(29)–F(33)	112.3 (6)
N(17)–C(16)–C(18)	111.8 (4)	F(31)–B(29)–F(32)	106.0 (5)
C(16)–C(18)–C(19)	118.8 (4)	F(31)–B(29)–F(33)	107.8 (6)
C(16)–C(18)–C(20)	114.2 (4)	F(32)–B(29)–F(33)	110.4 (5)
C(19)–C(18)–C(20)	127.0 (5)	F(35)–B(34)–F(36)	107.4 (12)
N(20)–C(21)–C(22)	110.6 (4)	F(35)–B(34)–F(37)	113.7 (17)
C(21)–C(22)–C(23)	104.6 (5)	F(35)–B(34)–F(38)	107.8 (16)
C(21)–C(22)–C(23′)	102.0 (5)	F(36)–B(34)–F(37)	103.7 (16)
C(22)–C(23)–C(24)	132.0 (9)	F(36)–B(34)–F(38)	114.4 (19)
C(22)–C(23′)–C(24′)	134.8 (8)	F(37)–B(34)–F(38)	109.9 (14)
C(22)–C(23)–C(28)	117.3 (8)	F(35′)–B(34′)–F(36′)	100.4 (21)
C(22)–C(23′)–C(28′)	116.9 (7)	F(35′)–B(34′)–F(37′)	105.8 (15)
C(24)–C(23)–C(28)	110.7 (9)	F(35′)–B(34′)–F(38′)	109.8 (15)
C(24′)–C(23′)–C(28′)	108.3 (8)	F(36′)–B(34′)–F(37′)	101.4 (30)
C(23)–C(24)–C(25)	132.7 (11)	F(36′)–B(34′)–F(38′)	120.2 (39)
C(23′)–C(24′)–C(25)	131.6 (10)	F(37′)–B(34′)–F(38′)	117.1 (20)

[a] Estimated standard deviations in the least significant figure are given in parentheses.

Table VII. Selected Bond Distances (Å) in $[Cu^{II}((imidH)_2DAP)](BF_4)_2$[a]

Cu–N(1)	1.99 (1)	C(11)–N(16)	1.35 (2)
Cu–N(8)	2.05 (1)	C(12)–C(13)	1.32 (3)
Cu–N(16)	1.93 (1)	C(13)–C(14)	1.37 (3)
Cu–N(19)	2.09 (1)	C(14)–C(15)	1.39 (3)
Cu–N(26)	2.20 (2)	C(15)–N(16)	1.29 (2)
N(1)–C(2)	1.36 (3)	C(15)–C(17)	1.49 (3)
N(1)–C(5)	1.34 (2)	C(17)–C(18)	1.52 (3)
C(2)–N(3)	1.35 (2)	C(17)–N(19)	1.24 (3)
N(3)–C(4)	1.32 (3)	N(19)–C(20)	1.49 (3)
C(4)–C(5)	1.35 (3)	C(20)–C(21)	1.46 (3)
C(5)–C(6)	1.46 (3)	C(21)–C(22)	1.50 (3)
C(6)–C(7)	1.54 (3)	C(22)–C(23)	1.36 (3)
C(7)–N(8)	1.43 (2)	C(22)–N(26)	1.34 (2)
N(8)–C(9)	1.27 (2)	C(23)–N(24)	1.32 (3)
C(9)–C(10)	1.48 (3)	N(24)–C(25)	1.36 (3)
C(9)–C(11)	1.41 (3)	C(25)–N(26)	1.36 (3)
C(11)–C(12)	1.48 (3)		

[a] Estimated standard deviations in the least significant figure are given in parentheses.

Table VIII. Selected Bond Angles (deg) in $[Cu^{II}((imidH)_2DAP)](BF_4)_2$[a]

N(1)–Cu–N(8)	92.4 (6)	C(9)–C(11)–N(16)	117 (2)
N(1)–Cu–N(16)	151.2 (6)	C(12)–C(11)–N(16)	116 (2)
N(1)–Cu–N(19)	107.1 (6)	C(11)–C(12)–C(13)	116 (2)
N(1)–Cu–N(26)	98.1 (6)	C(12)–C(13)–C(14)	124 (2)
N(8)–Cu–N(16)	80.3 (6)	C(13)–C(14)–C(15)	119 (2)
N(8)–Cu–N(19)	157.5 (6)	C(14)–C(15)–N(16)	119 (2)
N(8)–Cu–N(26)	107.4 (6)	C(14)–C(15)–C(17)	129 (2)
N(16)–Cu–N(19)	77.1 (6)	N(16)–C(15)–C(17)	112 (2)
N(16)–Cu–N(26)	110.7 (6)	Cu–N(16)–C(11)	114 (1)
N(19)–Cu–N(26)	81.5 (6)	Cu–N(16)–C(15)	120 (1)
Cu–N(1)–C(2)	128 (1)	C(11)–N(16)–C(15)	126 (2)
Cu–N(1)–C(5)	122 (1)	C(15)–C(17)–C(18)	117 (2)
C(2)–N(1)–C(5)	110 (1)	C(15)–C(17)–N(19)	116 (2)
N(1)–C(2)–N(3)	102 (2)	C(18)–C(17)–N(19)	127 (2)
C(2)–N(3)–C(4)	115 (2)	Cu–N(19)–C(17)	115 (1)
N(3)–C(4)–C(5)	104 (2)	Cu–N(19)–C(20)	123 (1)
N(1)–C(5)–C(4)	109 (2)	C(17)–N(19)–C(20)	121 (2)
N(1)–C(5)–C(6)	121 (2)	N(19)–C(20)–C(21)	111 (2)
C(4)–C(5)–C(6)	130 (2)	C(20)–C(21)–C(22)	115 (2)
C(5)–C(6)–C(7)	114 (2)	C(21)–C(22)–C(23)	126 (2)
C(6)–C(7)–N(8)	112 (1)	C(21)–C(22)–N(26)	124 (2)
Cu–N(8)–C(7)	123 (1)	C(23)–C(22)–N(26)	109 (2)
Cu–N(8)–C(9)	113 (1)	C(22)–C(23)–N(24)	104 (2)
C(7)–N(8)–C(9)	124 (1)	C(23)–N(24)–C(25)	114 (2)
N(8)–C(9)–C(10)	122 (2)	N(24)–C(25)–N(26)	103 (2)
N(8)–C(9)–C(11)	116 (2)	Cu–N(26)–C(22)	116 (1)
C(10)–C(9)–C(11)	122 (2)	Cu–N(26)–C(25)	134 (1)
C(9)–C(11)–C(12)	127 (2)	C(22)–N(26)–C(25)	110 (2)

[a] Estimated standard deviations in the least significant figure are given in parentheses.

fashion. The helical configuration of the ligand about the metal makes the Cu(I/II) ions chiral centers. Like previously reported structures in the series, $[Cu^{II}((5\text{-MeimidH})_2DAP)](BF_4)_2$ crystallized as a racemic mixture of both the $\Lambda(\delta,\delta)$ and $\Delta(\lambda,\lambda)$ isomers. The nonprimed and primed orientations, as displayed in the disorder model in Figure 4, define the Λ and Δ configurations, respectively. In Figure 5, the complex is depicted in the Λ configuration with the two six-membered chelate rings in δ conformations. Similarly, the $[Cu^{II}((imidH)_2DAP)]^{2+}$ cation in Figure 6 is illustrated as the $\Lambda(\delta\delta)$ isomer.

Despite the similarities mentioned above, the coordination polyhedra of these structures are best described in somewhat different terms. Goodwin et al. described the coordination geometries of $[Cu^{I}((imidH)_2DAP)](BF_4)$ and $[Cu^{I}((py)_2DAP)](BF_4)$ as quasi trigonal bipyramidal.[6,7] Long Cu–N(imine) bonds (Table IX) define the unique axis of the polyhedra, while the central pyridine nitrogen and the terminal ring nitrogens define the trigonal plane as shown in Figure 7. In contrast, $[Cu^{II}((imidH)_2DAP)](BF_4)_2$ and $[Cu^{II}((py)_2DAP)](BF_4)_2$[6] lie nearly at the opposite extreme with their coordination spheres being more like distorted square pyramids. In these structures, the two terminal chelate rings are distinct and only one choice for the unique square-pyramidal axial ligand is appropriate. The longer Cu–N(terminal ring) bond defines the axial ligand, while the other

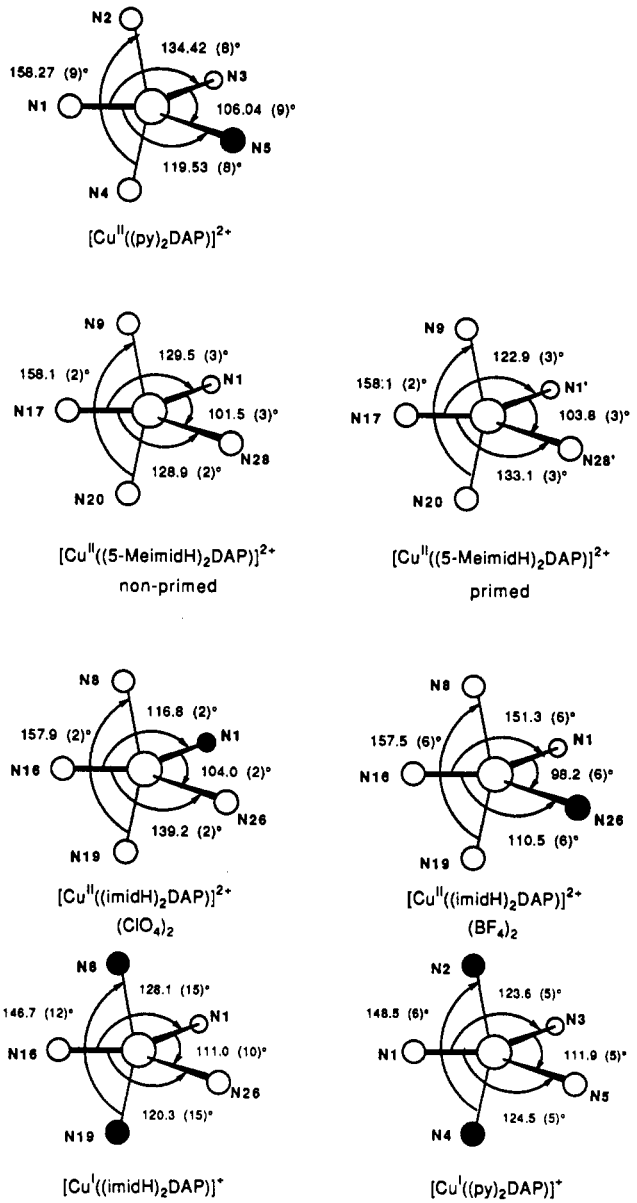

Figure 7. Selected bond angles within the inner coordination sphere of the Cu(I/II) cations. The shaded spheres define the axial positions of the polyhedra.

Table IX. Comparison of Cu–N Distances (Å) in the $[Cu^{II}((5\text{-MeimidH})_2DAP)]^{2+}$, $[Cu^{I/II}((imidH)_2DAP)]^{n+}$, and $[Cu^{I/II}((py)_2DAP)]^{n+}$ Structures

	nitrogen atom			
complex	central pyridine	terminal rings	imine	av[a]
$[Cu^{II}((5\text{-MeimidH})_2DAP)](BF_4)_2$ nonprimed[b]	1.924 (4)	2.036 (8) 2.066 (8)	2.058 (4) 2.013 (4)	2.019
$[Cu^{II}((5\text{-MeimidH})_2DAP)](BF_4)_2$ primed[b]	1.924 (4)	2.045 (9) 2.017 (8)	2.058 (4) 2.013 (4)	2.011
$[Cu^{II}((imidH)_2DAP)](BF_4)_2$[b]	1.93 (1)	1.99 (1) 2.19 (2)	2.05 (1) 2.09 (1)	2.05
$[Cu^{II}((imidH)_2DAP)](ClO_4)_2$[c]	1.923 (5)	2.081 (6) 1.992 (5)	2.066 (5) 2.036 (6)	2.020
$[Cu^{I}((imidH)_2DAP)](BF_4)$[d]	1.895 (33)	1.887 (29) 1.933 (31)	2.282 (31) 2.534 (29)	2.106
$[Cu^{II}((py)_2DAP)](BF_4)_2$[e]	1.920 (2)	2.033 (2) 2.129 (2)	2.010 (2) 2.026 (2)	2.024
$[Cu^{I}((py)_2DAP)](BF_4)_2$[e]	2.094 (14)	2.032 (12) 2.083 (12)	2.273 (14) 2.240 (14)	2.144

[a] Average of five values. [b] This work. [c] From ref 9. [d] From ref 7. [e] From ref 6.

Table X. Dihedral Angle (deg) Comparisons in the $[Cu^{I/II}((py)_2DAP)]^{n+}$, $[Cu^{I/II}((imidH)_2DAP)]^{n+}$, and $[Cu^{II}((5\text{-}MeimidH)_2DAP)]^{2+}$ Structures

	interplanar angles						
						Cu^{II}(5-Me)	
planes[a]	Cu^{I}(py)[b]	Cu^{II}(py)[b]	Cu^{I}(imidH)[c]	Cu^{II}(imidH)$(ClO_4)_2$[d]	Cu^{II}(imidH)$(BF_4)_2$[e]	nonprimed[e]	primed[e]
1–2	64.1	68.8	62.0	75.8	81.0	76.8	68.0
1–3	68.5	66.5	64.3	54.1	46.7	68.1	71.6
1–4	67.8	66.2	65.7	54.1	46.2	68.3	71.3
1–5	71.3	67.4	78.5	71.4	75.1	65.7	63.2
2–3	75.5	81.1	84.4	77.4	80.1	71.6	78.7
2–4	75.3	80.9	84.8	77.5	79.3	71.8	78.5
2–5	74.7	63.5	70.1	65.8	65.3	63.6	69.0
3–4	1.4	0.5	2.2	0.1	1.1	0.4	0.4
3–5	69.2	76.8	63.1	78.3	75.0	77.2	74.0
4–5	70.5	77.3	61.0	78.2	76.1	76.8	74.5

[a] Refer to Table S-VI (supplementary material) for the calculated least-squares planes. Plane 1: N(1), C(2), N(3), C(4), C(5). Plane 2: C(22), C(23), N(24),C(25), N(26). Plane 3: C(7), N(8), C(9), C(10), C(11), C(12), C(13), C(14), C(15), N(16), C(17), C(18), N(19), C(20). Plane 4: N(8), C(9), C(10), C(11), C(12), C(13), C(14), C(15), N(16), C(17), C(18), N(19). Plane 5: N(1), N(16), N(26). [b] From ref 6. [c] From ref 7. [d] From ref 9. [e] This work.

four nitrogen donor atoms defines the basal plane. A similar square-pyramidal description of the coordination group for $[Cu^{II}((imidH)_2DAP)](ClO_4)_2$ seems equally valid.[6] Finally, the coordination sphere of $[Cu^{II}((5\text{-}MeimidH)_2DAP)](BF_4)_2$ (primed and nonprimed) is seemingly best described as intermediate between a square pyramid and a trigonal bipyramid. Unlike the other Cu(II) cations, there is no significant difference in the two Cu–N(terminal ring) bond distances; therefore; it is not possible to assign a unique axial ligand position.

In previous work, the dihedral angles between equivalent least-squares planes were compared to show the difference in the detailed orientations of the polyhedra as a function of oxidation state.[6,7] For example, in the $[Cu^{I/II}((py)_2DAP)]^{+/2+}$ structures, the dihedral angles (Table X) were 2.0 and 1.6° smaller for Cu(II) between planes 1–3 and 1–4, respectively and 5.6° greater for Cu(II) between both the 2–3 and 2–4 planes. For the $[Cu^{I/II}((imidH)_2DAP)]^{+/2+}$ structures, the dihedral angles were 10.2, 11.6, 4.2, and 5.6° smaller for Cu(II) between planes 1–3, 1–4, 2–3, and 2–4, respectively. For the present $[Cu^{II}((imidH)_2DAP)]^{2+}$ crystal structure, a comparison of the dihedral angles between equivalent planes can be made for the same Cu(II) cation in two environments (the counterions being ClO_4^- for one structure and BF_4^- for the other). The dihedral angles are 7.4 and 7.9° smaller for the BF_4^- structure between planes 1–3 and 1–4, respectively, and 2.7 and 1.8° greater between planes 2–3 and 2–4, respectively. Thus, differences in the dihedral angles between the two $[Cu^{II}((imidH)_2DAP)]^{2+}$ structures are as large as those observed between the Cu(I) and Cu(II) oxidation states. Moreover, a comparison of the dihedral angles between equivalent planes in the $[Cu^{II}((5\text{-}MeimidH)_2DAP)]^{2+}$ structure, where there is the same ligand, oxidation state, and counterion, shows that there are genuine differences in the detailed orientations of the two disordered molecules (labeled as primed and nonprimed, Figure 4). Taken together, the above observations suggest that the details of molecular structure in the solid state for these pentacoordinate species are strongly influenced by crystal lattice forces as well as by changes in oxidation state.

Solution-State Structure. Copper K-edge EXAFS data on $[Cu^{I,II}((imidH)_2DAP)]^{+/2+}$ have been reporteed.[8] In the Cu(II) complex, five N atoms were accounted for at a distance of 2.00 Å (the crystallographic average is 2.02 Å). In the Cu(I) case, three N atoms were accounted for at an average distance of 1.91 Å with the two other N atoms at 2.40 Å, which is also near the crystallographic averages of the bond distances. Thus, the EXAFS data are consistent with a model in which the solution- and solid-state structures are very similar.[8] Although EXAFS data for the other Cu(I/II) compounds are not available at this time, it is assumed that a similar relationship exists between the solid-state and solution-state structures. In addition, the proton NMR results for all of the Cu(I) derivatives indicate that the predominant species in solution is pentacoordinate and of effective C_2 symmetry.[6,8,28]

Table XI. Electron Self-Exchange Rate Constants in CD_3CN for the Pentacoordinate Copper Complexes

complex	$10^3 k_{ex}$, M^{-1} s^{-1}	μ, mM[a]	T, K
$[Cu^{II/I}((py)_2DAP)]^{2+/+}$	k'_{11} = 1.76 (0.16)[b]	50	298
$[Cu^{II/I}((imidH)_2DAP)]^{2+/+}$	k'_{22} = 13.1 (1.6)[c]	22	298
$[Cu^{II/I}((imidR)_2DAP)]^{2+/+}$[d]	k'_{33} = 24.3[e]	38	298
$[Cu^{II/I}((5\text{-}MeimidH)_2DAP)]^{2+/+}$	k'_{44} = 35.3 (6.1)[f]	25	293

[a] Ionic strength (Me_4NBF_4). [b] Direct measurement; from ref 6. [c] Direct measurement; from ref 8. [d] R group is *p*-xylyl. [e] Calculated by applying the Marcus cross relationship, from ref 7. [f] Direct measurement; this work.

Electron Self-Exchange Studies for Small-Molecule Cu(I/II) Systems. The mechanism of electron transfer for the present series of $[Cu^{I/II}((arm)_2DAP)]^{+/2+}$ redox couples is believed to be outer sphere,[8] but there is still uncertainty as to whether this is the case. As previously reported by Goodwin et al., if ion-pairing contributions are disregarded, the rate laws for the cross-exchange reactions of $[Cu^{II}((py)_2DAP)]^{2+}$ with $[Cu^{I}((imidH)_2DAP)]^{+}$ and with $[Cu^{I}((imidR)_2DAP)]^{+}$ (R = *p*-xylyl) imply a simple bimolecular mechanism.[6,8] Because the $((arm)_2DAP)$ ligands do not provide any lone pairs of electrons for bridging, a simple inner-sphere mechanism seems unlikely. However, it is conceivable that an arm of one ligand could dissociate from its Cu(I) center, rotate, and bind to an adjacent Cu(II) center in concert with electron transfer. A process such as this would provide a bridge containing a saturated ethylene linkage for an inner-sphere mechanism. The arm dissociation rate constant, k_d, for $[Cu^{I}((py)_2DAP)]^{+}$ has been found to be 310 s^{-1} by ligand substitution kinetics with $[Zn^{II}(CH_3CN)_6]^{2+}$,[8] and as we have previously demonstrated, a dissociation rate of this magnitude is large enough for the electron-transfer reaction to proceed through an inner-sphere mechanism.[8] However, it is not clear why an inner-sphere mechanism would confer any kinetic advantage relative to an outer-sphere one. In addition, an outer-sphere mechanism might be anticipated because of the relatively small structural differences between the pentacoordinate structures in their different oxidation states and the ample opportunity for adiabatic overlap. The final analysis of the electron-transfer mechanism for these pentacoordinate Cu(I/II) complexes must await further experimental evaluation, but for now, an outer-sphere mechanism continues to be favored.

The self-exchange rate constant for $[Cu^{I,II}((5\text{-}MeimidH)_2DAP)]^{+/2+}$ is similar in magnitude to those observed for the other imidazole-containing derivatives and is 20-fold greater than that observed for the $[Cu^{I,II}((py)_2DAP)]^{+/2+}$ complex (Table XI). The fact that k'_{33} and k'_{44} are greater than k'_{11} can be rationalized on the basis that solvent reorganization energies decrease with increased ligand bulk. However, solvation effects cannot account for the fact that k'_{22} is a factor of 7 greater than k'_{11}. Recently, we proposed that the mechanism of electron-transfer reaction for these redox couples may involve sequential conformational change

and electron transfer.[8] This proposal was based upon an inspection of the structural changes for the $[Cu^{I,II}((py)_2DAP)]^{+/2+}$ and $[Cu^{I,II}((imidH)_2DAP)]^{+/2+}$ redox couples as a function of oxidation state. In the former case, the central pyridine and the two imine nitrogens were seen to move as a unit with the change in oxidation state. In the latter redox system, the motion appeared more complex, with features that might be described as conformational in character. This suggested that a different conformation of only slightly increased energy may exist for one of the oxidation states so that the structural difference between it and the other oxidation state is relatively small. The present crystal structure shows that $[Cu^{II}((imidH)_2DAP)]^{2+}$ does indeed have at least two significantly different low-energy geometries. As Brunschwig and Sutin have recently pointed out, the existence of such low-energy conformational isomers does not require a sequential mechanism.[37] Moreover, they have shown that such isomers can enhance the rates even in the case of direct electron transfer. Our present view is that the potential energy surfaces for our copper systems are relatively flat, so that it is difficult to draw a direct correlation between the degree of structural change and the electron-exchange rate.

The results of our concurrent NMR investigation[28] of the ligand mobility of these Cu(I) complexes is pertinent to these issues, since the coalescence temperatues for $[Cu^{I}((5\text{-MeimidH})_2DAP)]^{+}$ ($T_c \approx 203$ K) and $[Cu^{I}((py)_2DAP)]^{+}$ ($T_c \approx 253$ K) in CD_2Cl_2 indicate that the former compound is more mobile. Thus, $[Cu^{I}((5\text{-MeimidH})_2DAP)]^{+}$, which has the greater self-exchange rate, is more mobile than $[Cu^{I}((py)_2DAP)]^{+}$, and it is possible that the coordination-sphere reorganization processes within the electron-transfer association complex could parallel this molecular dynamics. Unfortunately, coalescence temperatures are not yet available for the other two Cu(I) complexes in the series. Additional data must be obtained before firm conclusions can be drawn as to whether a correlation actually exists between ligand conformational mobility in these Cu(I) complexes and the rate of electron self-exchange, but such a connection does not seem unreasonable. In a recent investigation of the electron-transfer cross-reactions for a series of Cu(I/II) polythia ether complexes, Martin et al. have presented a "square" scheme in which a major portion of the conformational reorganization at the copper centers occurs sequentially, rather than concertedly, with electron transfer.[10] Evidence for such a scheme comes from cyclic voltammetric measurements on the copper complexes.[38] They also postulate that the NMR spectrum of the $[Cu^{I}([14]aneS_4)]^{+}$ complex ([14]aneS$_4$ = 1,4,8,11-tetrathiacyclotetradecane) indicates that the four S donors are equivalent and that two alternate forms of the Cu(I) complex are interconverting slowly on the NMR time scale.

Because the self-exchange rate for the present $[Cu((5\text{-MeimidH})_2DAP)]^{+/2+}$ couple has been studied as a function of temperature, activation parameters for one of the pentacoordinate systems has been obtained for the first time. To date, direct measurements of k_{ex} for small-molecule Cu(I/II) couples have been reported for nine compounds,[6,8,12,13,24-26] and, of these, only two have reported activation parameters as well as rate constants: (i) $[Cu(bidhp)]^{+/2+}$ in DMSO-d_6;[13] (ii) $[Cu(dmp)_2]^{+/2+}$ in D_2O, CD_3CN, and acetone-d_6.[25] It is not certain that either of these two reactions does not involve a change in coordination number. Thus, to assess the prevent activation parameters with respect to bona fide outer-sphere coordination-number-invariant electron-transfer reactions in acetonitrile, we are forced to consider complexes other than those of copper. The $[Mn(CNR)_6]^{2+/+}$ complexes studied in CD_3CN by Nielson and Wherland provide just such a comparison.[39,40] These self-exchange reactions have values of $\Delta S^{\ddagger}$ in the range from −18 to −24 cal mol^{-1} K^{-1}, and our value of −25 cal mol^{-1} K^{-1} is close enough to indicate that this result may be typical of such reactions. Thus, rate differences for such reactions should be reflected primarily in $\Delta H^{\ddagger}$.

Table XII. Electron Self-Exchange Rate Constants and the Corresponding Activation Parameters for the Three Small-Molecule Copper Complexes

solvent; T, K	$\Delta H^{\ddagger}$, kJ mol^{-1}	$\Delta S^{\ddagger}$, J K^{-1} mol^{-1}	k_{ex}
	$[Cu((5\text{-MeimidH})_2DAP)]^{+/2+}$		
CD_3CN; 293	16.2 (3.3)	−103 (12)	3.5 (0.6) × 10^{4} [a,b]
	$[Cu(bidhp)]^{+/2+}$		
DMSO-d_6; 301	38.1 (2.5)	−49.4 (6.7)	3.8 (0.2) × 10^{3} [a,c]
	$[Cu(dmp)_2]^{+/2+}$		
CD_3CN; 298	29.6 (0.8)	−75 (3)	4.9 (0.2) × 10^{3} [d,e]
acetone-d_6; 298	29.2 (0.6)	−80 (2)	3.0 (0.2) × 10^{3} [d,e]
D_2O; 298	24 (3)	−63 (10)	2.0 (0.2) × 10^{5} [d,e]

[a] Units are M^{-1} s^{-1}. [b] This work. [c] From ref 13. [d] Units are kg mol^{-1} s^{-1}. [e] From ref 25.

Comparisons of the activation parameters for the copper complexes must remain qualitative because solvent and ionic strength are variables. However, inspection of the data in Table XII reveals that $[Cu(dmp)_2]^{+/2+}$ and $[Cu(bidhp)]^{+/2+}$ have similar rate constants in nonaqueous solvents, whereas k_{ex} for $[Cu((5\text{-MeimidH})_2DAP)]^{+/2+}$ is an order of magnitude greater (10^4 versus 10^3). Since $\Delta S^{\ddagger}$ (−103 J K^{-1} mol^{-1}) for the present pentacoordinate complex is large and unfavorable, the increase in k_{ex}, compared to that for the other small-molecule systems, is due to a relatively small and favorable $\Delta H^{\ddagger}$ term (12 kJ mol^{-1}). Thus, while all three of the Cu(I/II) systems exhibit relatively fast and comparable electron self-exchange kinetics (10^3–10^4 M^{-1} s^{-1}) in nonaqueous solvents, the magnitudes of the rate constants have considerably different origins. The reason for this difference is not yet clear, but it may be related to the possibility that only the $[Cu^{I,II}((5\text{-MeimidH})_2DAP)]^{+/2+}$ couple has the same coordination number in both oxidation states.

Finally, it is of interest to compare the present small-molecule results with those obtained for azurin from *Pseudomonas aeruginosa*. It has been argued that in the azurin self-exchange reaction (k_{ex} = 1.2 (1) × 10^6 M^{-1} s^{-1} at 309 K),[41] the redox partners "dock" along the hydrophobic patch on the protein surface around the His-117 ligand. This argument was supported by the very strong dependence of the activation parameters on the nature of the buffer and pH; especially important in this deduction was the statistically significant compensation effect between $\Delta H^{\ddagger}$ and $\Delta S^{\ddagger}$. For these reasons it is diffult to assess from these data the contribution of reorganization at the copper center to the electron exchange rate in azurin. Thus, small-molecule studies such as in the present work should become important in exposing the nature of the copper-containing active site itelf, in effect factoring out its contribution to the overall protein electron-transfer reactivity. *The present results raise the suggestion that, with appropriate ligands, the potential-energy surfaces of copper complexes can be rather flat, which can lead to low inner-sphere Franck–Condon barriers to self-exchange in cuproproteins.* Future small-molecule studies, of careful design, may permit confirmation of this suggestion.

Conclusions. The electron self-exchange properties of the $[Cu^{I,II}((5\text{-MeimidH})_2DAP)]^{+/2+}$ redox pair have been studied in CD_3CN by dynamic NMR line-broadening methods to yield rate constants on the order of 10^4 M^{-1} s^{-1}. The $[Cu^{II}((5\text{-MeimidH})_2DAP)]^{2+}$ cation has been shown to be pentacoordinate in the solid state, and it is likely that the analogous Cu(I) compound is also pentacoordinate, as is its $[Cu^{I}((imidH)_2DAP)]^{+}$ parent compound. Thus, the electron self-exchange reaction in solution occurs between small-molecule Cu(I) and Cu(II) compounds in which there is no change in coordination number. Previous electron self-exchange and cross-exchange studies on related Cu(I/II) systems[6,8] have indicated an outer-sphere electron-

(37) Brunschwig, B. S.; Sutin, N. *J. Am. Chem. Soc.* **1989**, *111*, 7454–7465.
(38) Bernardo, M. M.; Robandt, P. V.; Schroeder, R. R.; Rorabacher, D. B. *J. Am. Chem. Soc.* **1989**, *111*, 1224–1231.
(39) Nielson, R. M.; Wherland, S. *J. Am. Chem. Soc.* **1985**, *107*, 1505–1510.
(40) Nielson, R. M.; Wherland, S. *Inorg. Chem.* **1984**, *23*, 1338–1344.
(41) Groeneveld, C. M.; Canters, G. W. *Eur. J. Biochem.* **1985**, *153*, 559–564.

transfer mechanism for this class of pentacoordinate compounds. Available data now suggest that there may exist a relationship between the rate of intramolecular conformational mobility in the Cu(I) compounds and the rate of electron self-exchange between the Cu(I/II) pairs. Finally, the study of the self-exchange rate constant for $[Cu^{I,II}((5\text{-MeimidH})_2DAP)]^{+/2+}$ as a function of temperature is the first such study for these pentacoordinate complexes. The activation parameters indicate that the relatively large self-exchange rate constant ($k'_{44} = 3.5 \times 10^4$ M^{-1} s^{-1} at 293 K) is dominated by an unusually favorable ΔH^* (16 kJ mol^{-1}) contribution.

Acknowledgment. At Rice University, this work was supported by National Institutes of Health Grant GM-28451 from The National Institute of General Medical Science and Grant C-624 from The Robert A. Welch Foundation. Work at the University of Notre Dame was supported by National Institutes of Health Grant GM-38401. The Rigaku AFC-5S X-ray diffractometer, at Rice, was purchased, in part, through an instrumentation grant from The National Science Foundation.

Supplementary Material Available: Tables S-II, S-IV, and S-V, listing final anisotropic thermal parameters, fixed hydrogen atom coordinates, and rigid group parameters, respectively, for $[Cu^{II}((imidH)_2DAP)](BF_4)_2$, and Table S-VI, listing the calculated least-squares planes (6 pages); Tables S-I and S-III, listing observed and calculated structure amplitudes (×10) for $[Cu^{II}((5\text{-MeimidH})_2DAP)](BF_4)_2 \cdot {}^1/_2CH_3OH$ and $[Cu^{II}((imidH)_2DAP)](BF_4)_2$ (30 pages). Ordering information is given on any current masthead page.

Contribution from Ames Laboratory and the Department of Chemistry, Iowa State University, Ames, Iowa 50011

Oxidative Homolysis of Organochromium Macrocycles

Carl R. Steffan, James H. Espenson,* and Andreja Bakac*

Received August 24, 1990

The complexes $RCrL(H_2O)^{2+}$ (R = alkyl, aralkyl; L = 1,4,8,12-tetraazacyclopentadecane) are oxidized by $Ru(bpy)_3^{3+}$ and ^2E $Cr(bpy)_3^{3+}$. The one-electron oxidized species $RCrL(H_2O)^{3+}$ undergoes subsequent homolysis; the R• radicals so produced may react with certain metal complexes, or they dimerize, depending on conditions. The rate constants for the rate-controlling step, electron transfer from $RCrL(H_2O)^{2+}$ to $Ru(bpy)_3^{3+}$ or $*Cr(bpy)_3^{3+}$, were measured by laser flash photolysis for an extensive range of R groups. For $Ru(bpy)_3^{3+}$, the rate constants range from 14.2 L mol^{-1} s^{-1} (R = CH_3) to 1.05×10^9 (R = 4-$CH_3C_6H_4CH_2$); for $*Cr(bpy)_3^{3+}$, the corresponding values are 2.8×10^6 and 1.55×10^9 L mol^{-1} s^{-1}. In both series, the order of rate constants is methyl < primary alkyl < secondary alkyl < aralkyl. The plots of log k versus the gas-phase ionization potentials of R• are linear, in accord with the rate-controlling step being electron transfer.

Introduction

One-electron oxidation of an organometal (L_nMR) leads to an oxidized species (L_nMR^+) whose fate is often but not always homolysis ($\rightarrow L_nM^+ + R^\bullet$). This process, collectively termed oxidative homolysis, has been examined for a considerable number of organometals. This includes the oxidation of R_4Pb (R = CH_3, C_2H_5)[1,2] and R_2Hg[3] by $IrCl_6^{2-}$, oxidative coupling of $R_2Fe(bpy)_2$[4,5] and $R_2Ni(bpy)$[4] and oxidation of R_4Sn[6-8] and $R_2Pt(PPh_3)_2$.[9] Considerable effort has also been devoted to the oxidation of $RCo(dmgH)_2H_2O$ and its numerous Schiff-base analogues.[10-30]

The present study arises from previous work dealing with the oxidation of $(H_2O)_5CrR^{2+}$ and $RCrL(H_2O)^{2+}$ (L = 1,4,8,12-tetraazacyclopentadecane) complexes.[31-35] In the pentaaqua series, oxidants include $Ni([14]aneN_4)^{3+}$, $Ru(bpy)_3^{3+}$, NO^+, and

(1) Gardner, H. C.; Kochi, J. K. *J. Am. Chem. Soc.* **1974**, *96*, 1982.
(2) Gardner, H. C.; Kochi, J. K. *J. Am. Chem. Soc.* **1975**, *97*, 1855.
(3) Chen, J. Y.; Gardner, H. C.; Kochi, J. K. *J. Am. Chem. Soc.* **1976**, *98*, 6150.
(4) Tsou, T. T.; Kochi, J. K. *J. Am. Chem. Soc.* **1978**, *100*, 1634.
(5) Lau, W.; Huffman, J. C.; Kochi, J. K. *Organometallics* **1982**, *1*, 155.
(6) Fukuzumi, S.; Kuroda, S.; Tanaka, T. *J. Chem. Soc., Perkin Trans. 2* **1986**, 25.
(7) Wong, C. L.; Mochida, K.; Gin, A.; Weiner, M. A.; Kochi, J. K. *J. Org. Chem.* **1979**, *44*, 3979.
(8) Wong, C. L.; Kochi, J. K. *J. Am. Chem. Soc.* **1979**, *101*, 5593.
(9) Chen, J. Y.; Kochi, J. K. *J. Am. Chem. Soc.* **1977**, *99*, 1450.
(10) Vol'pin, M. E.; Levitin, I. Ya.; Sigan, A. L.; Nikitaev, A. T. *J. Organomet. Chem.* **1985**, *279*, 263.
(11) Levitin, I. Ya.; Sigan, A. L.; Vol'pin, M. E. *J. Organomet. Chem.* **1976**, *114*, C53.
(12) Tamblyn, W. H.; Klinger, R. J.; Hwang, W. S.; Kochi, J. K. *J. Am. Chem. Soc.* **1981**, *103*, 3161.
(13) Abley, P.; Dockal, E. R.; Halpern, J. *J. Am. Chem. Soc.* **1972**, *94*, 659.
(14) Halpern, J.; Chan, M. S.; Roche, T. S.; Tom, G. M. *Acta Chem. Scand., Ser. A* **1979**, *A33*, 141.
(15) Levitin, I. Ya.; Sigan, A. L.; Vol'pin, M. E. *J. Chem. Soc., Chem. Commun.* **1975**, 469.
(16) Halpern, J.; Chan, M. S.; Hanson, J.; Roche, T. S.; Topich, J. A. *J. Am. Chem. Soc.* **1975**, *97*, 1606.
(17) Topich, J.; Halpern, J. *Inorg. Chem.* **1979**, *18*, 1339.
(18) Halpern, J.; Topich, J.; Zamaraev, K. I. *Inorg. Chim. Acta* **1976**, *20*, L21.
(19) Anderson, S. N.; Ballard, D. H.; Chrzastowski, J. Z.; Dodd, D.; Johnson, M. D. *J. Chem. Soc., Chem. Commun.* **1972**, 685.
(20) Magnuson, R. H.; Halpern, J. *J. Chem. Soc., Chem. Commun.* **1978**, 44.
(21) Vol'pin, M. E.; Levitin, I. Ya.; Sigan, A. L. *Inorg. Chim. Acta* **1980**, *41*, 271.
(22) Roy, M.; Kumar, M.; Gupta, B. D. *Inorg. Chim. Acta* **1986**, *114*, 87.
(23) Gupta, B. D.; Kumar, M. *Inorg. Chim. Acta* **1988**, *149*, 223.
(24) Dreos, R.; Tauzher, G.; Marsich, N.; Costa, G. *J. Organomet. Chem.* **1976**, *108*, 235.
(25) Dreos, R.; Tauzher, G.; Marsich, N.; Costa, G. *J. Organomet. Chem.* **1975**, *92*, 227.
(26) Gupta, B. D.; Kumar, M. *Inorg. Chim. Acta* **1986**, *113*, 9.
(27) Gupta, B. D.; Roy, S. *Tetrahedron Lett.* **1984**, *25*, 3255.
(28) Okamoto, T.; Goto, M.; Oka, S. *Inorg. Chem.* **1981**, *20*, 899.
(29) Costa, G.; Puxeddu, A.; Tavagnacco, C.; Dreos-Garlatti, R. *Inorg. Chim. Acta* **1984**, *89*, 65.
(30) Reisenhofer, E.; Costa, G. *Inorg. Chim. Acta* **1981**, *49*, 121.
(31) Bakac, A.; Espenson, J. H. *J. Am. Chem. Soc.* **1988**, *110*, 3453.
(32) Katsuyama, T.; Bakac, A.; Espenson, J. H. *Inorg. Chem.* **1989**, *28*, 339.
(33) Melton, J. D.; Espenson, J. H.; Bakac, A. *Inorg. Chem.* **1986**, *25*, 4104.
(34) Melton, J. D.; Bakac, A.; Espenson, J. H. *Inorg. Chem.* **1986**, *25*, 3360.
(35) Shi, S.; Bakac, A.; Espenson, J. H. *Inorg. Chem.*, submitted for publication.

0020-1669/91/1330-1134$02.50/0